Journal of Mines, Metals and Fuels, *71(11): 2027-2037; 2023. DOI: 10.18311/jmmf/2023/36102*

Print ISSN : 0022-2755

Journal of Mines, Metals and Fuels

Contents available at: *www.informaticsjournals.com/index.php/jmmf*

Experimental Investigations and Quasi Dimensional Modelling of Spark Ignition Engine Fuelled with Gasoline and Oxyhydrogen Gas Mixture

K. R. Kirankumar[1], K. M. Manjunatha Swamy[2]* and H. Manjunath[2]

[1]*Department of Mechanical Engineering, National Institute of Technology Calicut, Kattangal - 673601, Kerala, India*
[2]*Department of Mechanical Engineering, Siddaganga Institute of Technology, Tumkur - 572103, Karnataka, India; manjukm11411@gmail.com*

Abstract

Oxy-hydrogen gas is a mixture of hydrogen and oxygen gas in 2:1 molar proportion. Oxy-hydrogen gas can be easily and economically produced from electrolysis of water by using dry cell electrolysers. Oxy-hydrogen gas is one of the alternative fuel options which can replace conventional fossil fuels like gasoline, diesel, etc., because of its high-octane number (>130) and moderate calorific value (21.4 MJ/kg). Current research work consists of both experimental and simulation parts. Experiments focussed on studying the performance and emission characteristics of spark ignition engine fuelled with gasoline (petrol) and dual fuel (gasoline + Oxy-hydrogen) mixture at variable load and constant speed condition with three different oxy-hydrogen flow rates. Comparative findings suggest that NOx emission and brake thermal efficiency increased by 1.75% and 800 PPM, respectively, at full load and at a flow rate of 1.54 lit/min. Carbon monoxide emission dropped by 0.25% at full load and at a flow rate of 1.54 lit/min. A two-zonequasi dimensional modelling of spark ignition engine was carried out in order to understand the combustion process efficiently. The predicted values accord well with the experimental data, with just a small variance. Commercially available software MATLAB R2021a is used to develop code for the engine simulation.

Keywords: *Dry Cell, Electrolysis, Emission, Oxy-Hydrogen, Performance, Phenomenological, Quasi*

1.0 Introduction

The need for energy is growing by the day due to increasing population and declining conventional fuel sources including fossil fuels. In the not-too-distant future, we can expect an energy crisis which includes fuels used for automobiles like petrol, diesel, etc. Other than the energy crisis we have to face other global threats like greenhouse effect, ozone layer depletion, and global warming. Some of the best alternative fuels are CNG, hydrogen, LPG, etc. But these fuels have their own limitations when it comes to their usage. Hydrogen is one of the best replacements because of its high-octane value and no carbon content. Mixtures of hydrogen and oxygen gas in stoichiometric ratio can be easily produced from electrolysis of water, this mixture is referred to as oxy-hydrogen gas. HHO gas is considered to be the best alternative fuel especially for SI engines because of its high-octane number. Lulianelli and Basile[1] studied the generation of HHO gas from the electrolysis of water and observed that the use of electrolytes such as NaOH or KOH increases the efficiency of the production of HHO gas. Santilli[2] found that KOH is a better electrolyte compared to NaOH for water electrolysis purposes. El Soly *et al.*,[3] conducted experiments on both dry and wet cell electrolyser and the results showed that dry cell electrolysers are far superior

**Author for correspondence*

than wet cell electrolyser because of their high HHO production rate and low electricity consumption. Nikolic *et al.*,[4] found that the use of chromium-cobalt activators enhances the efficiency of the production of HHO gas by 10% while maintaining other parameters the same. Apostolescu and Chiriac[5] used HHO gas in SI engines for the first time. Study suggested that there was a drop in BSFC, CO and UBHC but an increase in NO_x emission. Some researchers came up with contradictory results such as increment of NO_x emission with HHO addition. Kassaby *et al.*,[6] used relatively low flow rate of HHO gas in SI engine and he found that BTE and IMEP increment with increasing HHO flow rate. Subramanian *et al.*,[7] also suggested that at HHO flow rate of 2 lpm, BTE increased by 8% and all the emission parameters like NO_x, HC and CO_2 were reduced by an average amount of 50%. High knock tendency in two stroke SI engines is observed by the studies conducted by Rao and kumar[8]. First two zone quasi dimensional model developed by Poulos and Heywood[9], which developed based on turbulent modelling of flame propagation. First implementation of SI engine modelling in MATLAB was done by Buttsworth[10]. Blizard and Keck[11] developed a mass burn rate model which depends on entrainment theory unlike conventional turbulent model but this model suffers from lack of predictive capability at the end of combustion, where turbulence effect is almost nil. Tabaczynski *et al.*,[12] modified the entrainment model by adding an exponential factor, which makes the model better in predicting the mass burn rate even during the end of combustion phase. Wang *et al.*,[13] developed the more sophisticated model for laminar flame speed which can incorporate the effect of secondary fuel addition on flame growth. Yu *et al.*,[14] extended the similar kind of work on the mixture of hydrocarbon fuels.

A. Paykani *et al.*,[15] used a fractal based combustion model to simulate SI engine combustion. Since fractal models are very elegant in capturing the roughness of the flame front, the simulated mass burn rate was in excellent agreement with the experimental results. Ratnak Sok *et al.*,[16] used an improved turbulent burning velocity correlation based on flame kernel growth and turbulent length scale and the results showed better predictive capability of turbulent velocity compared to previous models. MATLAB commercial software was used for the modelling of SI engine combustion because of its user-friendly interface and it provides multiple inbuilt functions and plotting features, which makes the implementation of model very easy and effective.

2.0 Methodology of HHO Production

HHO gas is the mixture of oxygen and hydrogen, which can be produced from the electrolysis of water. Dry cell electrolyser was selected to produce HHO gas because of its low power consumption and high HHO productivity rate. Dry cell alone can't be coupled directly with the engine setup, it requires other devices like AC to DC converter, bubbler with silica gel, flame entrapper, unidirectional valves and connecting pipes. The whole water electrolyser

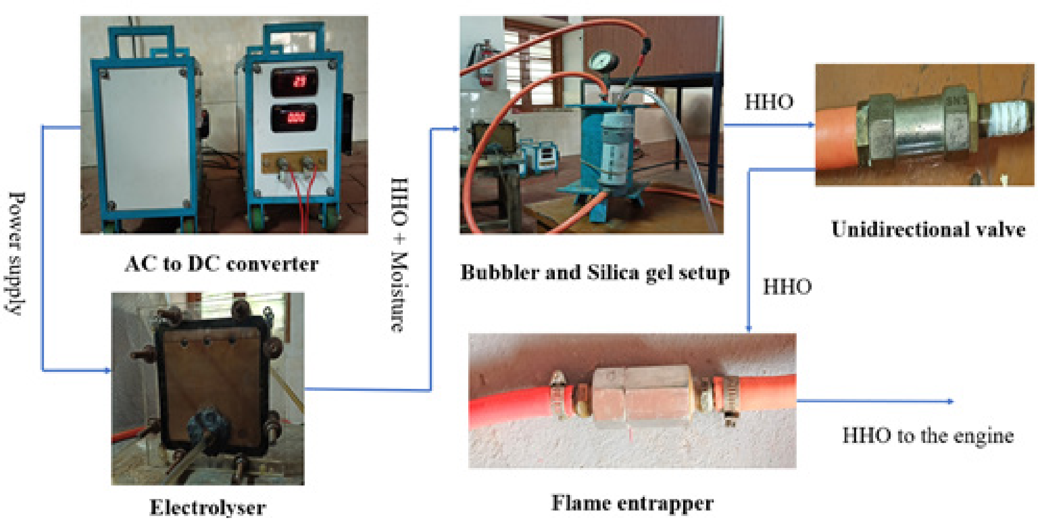

Figure 1. Experimental setup of water electrolyser.

setup is shown in Figure 1. Dry cell electrolyser consists of a series of steel plates and each plate is sandwiched between neoprene rubber to avoid short circuit. Two plates with a corner extension were randomly selected among the cluster of plates and connected to two different terminals of the power supply (AC to DC converter), depending upon the number of plates (neutral) available between the selected plates (electrodes) voltage should be maintained. 5, 8 and 10 sets of plates were only the combinations available corresponding to which minimum voltage of 10V, 16V and 20V of DC current was supplied by the converter. An average HHO production of 0.84, 1 and 1.54 lpm was produced by the above three combinations. HHO produced from the dry cell then circulated to bubbler, where bubbling effect takes place, which removes water vapor content in the gas mixture. Silica gel was also used to remove an extra moisture content in the HHO gas. For the safety of experiment flame entrapper and unidirectional valves were used. Flame entrapper avoids back flow of flame in the case of back fire from the engine and unidirectional valve was used to make sure that flow takes in one direction from water electrolyser setup to engine. All these components are connected by heat resistant flexible pipes.

3.0 Characteristics of HHO Gas

HHO (oxy-hydrogen gas) is also referred to as brown's gas, named after Yull Brown who generated the oxygen and hydrogen gas mixture from the electrolysis of water by using a wet cell electrolyser. Dry cell electrolyser was used to produce HHO gas for the current research work. HHO gas is a stoichiometric mixture of oxygen and hydrogen gas, whose properties lie in between the properties of individual constituent elements in terms of density, calorific value, etc. Table 1 represents a few important characteristics of HHO gas and gasoline.

HHO gas is the composition of oxygen and hydrogen, presence of these elements effects the combustion characteristics of SI engine. Hydrogen is a very highly diffusive gas and its laminar flame speed is far exceeding conventional fuels, because of these properties when HHO used along with gasoline in SI engine mass burn rate increases thus improves pressure and heat release rate, which in turn improves BTE of the engine. Oxygen reduces the fuel-air equivalence ratio of the fuel mixture, which helps in reduction of HC and CO emission. Only drawback of using HHO is its adverse effect on NO_x emission, presence of hydrogen in fuel mixture increases the flame burning temperature and causes increase in NO_x emission.

4.0 Experimental Setup and Procedure

4.1 Engine Test Rig

Both single (gasoline) and dual (gasoline +HHO) fuelled tests were done on a small 2 bhp, air cooled Honda GK-200 gasoline engine. Engine was loaded by using an electrical dynamometer and an energy meter associated with it, which is employed to determine bp of the engine at a particular load. Thermocouples were used to measure all important temperatures. Fuel and air flow rate were measured by using graduated burette and manometer setup respectively. Burette connected to fuel tank and water manometer connected to air box, which consists of orifice setup via flexible pipe. HHO gas flow rate can't be measured directly like air flow rate, instead it is measured by using a water displacement method. The speed of the engine was measured by using a digital tachometer in

Table 1. Properties of test fuels

Properties	Gasoline	Brown gas
Chemical formula	C_8H_{18}	HHO
Calorific value (MJ/kg)	44.45	21.995
Density (kg/m^3)	740.12	0.4911
Auto ignition temperature (^{o}C)	280	570
Octane number	91	>130

terms of rpm. The technical information about the engine is listed in Table 2. Exhaust species like CO, CO_2, NO_x, etc., were measured by using AVL DIgas 444 with RS232 gas analyser cable.

Table 2. Engine test rig specification

Parameters	Value
Bore	67 mm
Stroke length	56 mm
Connecting rod length	120 mm
Rated power	2 HP @ 3000 RPM
Cooling type	Air cooled
Loading device	Electrical dynamometer

4.2 Experimental Procedure

Experiments consist of two different parts, the former part focuses on pure gasoline fuelled engine while latter part focuses on gasoline and HHO fuelled engine. Total five loads were taken from no load (0%) to full load (100%) with an equal interval of 20% and at a fixed speed of 3000 rpm. Air flow rate is measured by reading the manometric height while fuel consumption rate is measured by taking time to consume 5 cc of fuel. Constant speed of 3000 RPM is ensured for each load by using a digital tachometer. Intake, exhaust and in cylinder temperatures were measured using thermocouples. If the engine runs on dual fuel (gasoline and HHO), then HHO flow rate is also an important factor, which can be calculated by using time taken to displace 250 cc of water in water displacement method. HHO gas was supplied to the engine at the air manifold by using a 1cm diameter pipe. Actual experimental setup with other accessories is shown in the Figure 2 below. Total three different flow rates of 0.84, 1 and 1.54 lpm were used during experimentation.

5.0 Engine Simulation Modelling

5.1 Combustion Process

Experiments suggest that combustion in SI engine consists of a smooth flame front originating from a spark plug and propagating towards an unburned mixture resulting in converting an unburned mixture of air-fuel into combustion product. Based on this argument a quasi-dimensional (phenomenological) model has been developed where the engine combustion chamber is divided into burned and unburned zones separated by a smooth hemispherical flame front. Generally, the flame front is not smooth because of turbulence associated with the combustion but to keep the model simple such kind of approximations are necessary. A schematic diagram representing a two-zone combustion model of SI engine is shown in the Figure 3 (Heywood[20]), where

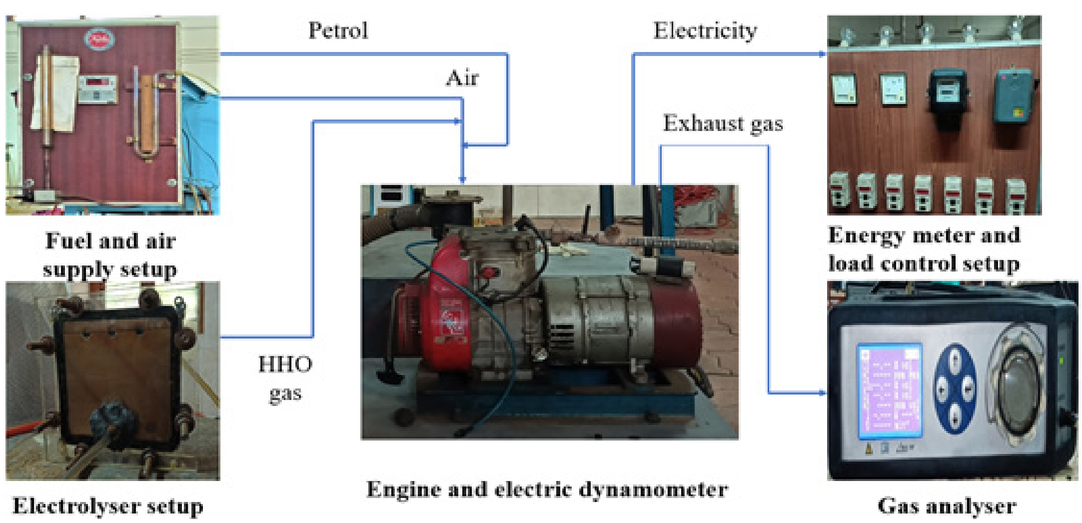

Figure 2. Experimental setup of SI engine.

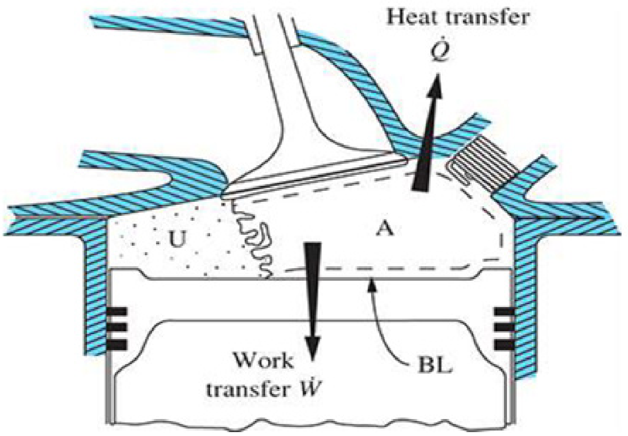

Figure 3. Schematic diagram of two zone combustion model in SI engine.

symbol 'U' and 'A' represents unburned and burned zone respectively. The differential Equations (1), (3), (4) and (7) were derived by considering whole combustion chamber as closed system but individual zones as open system. Following differential equations are derived by assuming working fluid as an ideal gas.

For unburned zone

$$\frac{dT_u}{dt} = \left(\frac{\frac{dQ_{wu}}{dt} + V_u\frac{dP}{dt}}{m_u C_{pu}}\right) \quad (1)$$

$$PV_u = m_u R_{gu} T_u \quad (2)$$

For burned zone

$$\frac{dT_b}{dt} = \left(\frac{\frac{dQ_{wb}}{dt} + V_b\frac{dP}{dt} + \frac{dm_b}{dt}(h_u - h_b)}{m_b C_{pb}}\right) \quad (3)$$

$$PV_b = m_b R_{gb} T_b \quad (4)$$

Pressure is considered to be uniform in both the zones, which is given by following Equation (5).

$$\frac{dP}{dt} = \left(P\left(\left(\frac{dm_b}{dt}\right)\left(\frac{1}{m_b}\right) + \left(\frac{dm_u}{dt}\right)\left(\frac{1}{m_u}\right) - \left(\frac{dV_u}{dt}\right)\right) + \left(\frac{\frac{dQ_{wu}}{dt}R_{gu}}{C_{pu}}\right) + \left(\frac{\left(\frac{dQ_{wb}}{dt} + \frac{dm_b}{dt}(h_u - h_b)\right)R_{gu}}{C_{pu}}\right)\right)(\zeta) \quad (5)$$

Where,

$$\zeta = \left(V - \left(\frac{V_u R_{gu}}{c_{pu}}\right) - \left(\frac{V_b R_{gb}}{c_{pb}}\right)\right)^{-1} \quad (6)$$

From the law of conservation of mass, relationship between unburned (m_u) and burned mass (m_b) is given by

$$\frac{dm_b}{dt} = -\frac{dm_u}{dt} \quad (7)$$

Initial temperature for unburned zone is the final temperature at the end of compression but initial temperature for burned zone is taken as adiabatic temperature which can be obtained from equating unburned enthalpy (h_u) and burned enthalpy (h_b) as given by the Equation (8).

$$\sum h_u = \sum h_b \quad (8)$$

Non combustion processes like compression and expansion follows same differential equation as above but with little modification. Equations (9) and (10) gives temporal variation of temperature and pressure for non-combustion processes.

$$\frac{dT}{dt} = \left(\frac{\frac{dQ_w}{dt} + V\frac{dP}{dt}}{mC_p}\right) \quad (9)$$

$$PV = mRT \quad (10)$$

In all the above equations we come across heat transfer rate ($\hat{Q}_w$) to wall, which is the crucial term which affects the modelling results. There are several models like Annand[17] Woschni, Eichelberg, etc., are present in the literature but the Woschni model [Ferguson *et al.*,[18]] is considered in the current research work because of its well predictive capability at both low and high temperature combustion. Heat transfer coefficient h_g expressed as a function of characteristic velocity, pressure, engine bore diameter and temperature.

$$h_g = 129.8p^{0.8}v^{0.8}D^{-0.2}T^{-0.55} \quad (11)$$

Where characteristic velocity (v) is given as

$$v = c_1 V_p + c_2(P - P_m)\left(\frac{V_d T_r}{p_r V_r}\right) \quad (12)$$

C_1 and C_2 are constants taken from Medina *et al.*[19]

5.2 Mass Burn Rate Model

Mass burn rate is a very important parameter on which a variety of parameters like pressure, temperature, etc., depends on. Since the combustion process is turbulent in nature, mass burn rate [Heywood[20]] is expressed in terms of turbulent velocity (S_T) given by Equation (13).

$$\frac{dm_b}{dt} = \rho_u A_f S_t \tag{13}$$

Where A_f is the hemispherical flame front area obtained by numerical method developed by medina *et al.*,[19]. Turbulent velocity expressed as the function of laminar speed (S_l) and given by the following equation

$$S_t = S_l f \left(\frac{\left(\frac{\rho_u}{\rho_b}\right)}{\left(\left(\frac{\rho_u}{\rho_b}\right) - 1\right) X_{m_b} + 1} \right) \tag{14}$$

Where f is a phenomenological turbulent factor, which depends several factors but, in our case, we consider it only depends on engine speed (N).

$$f = 1 + 0.0018N \tag{15}$$

Laminar flame speed (S_l) (equation16) is given by power law in terms of unburned temperature (T_u), pressure(P), unburned mass fraction (X_r) and relative amount of hydrogen present in fuel mixture (Y_{h2}).

$$S_l = S_{lo} \left(\frac{T_u}{T_{ref}}\right)^{(\alpha 1)} \left(\frac{p}{p_{ref}}\right)^{(\beta 1)} (1 - 2.06X_r^{0.77}) + 0.83y_{h2} \tag{16}$$

Where y_{h2} becomes zero for pure gasoline case. S_{lo},α and β are constants which can be expressed in terms of equivalence ratio (ϕ) taken from Heywood[20].

6.0 Results and Discussion

6.1 Performance and Emission

Comparative Performance analysis of single and dual fuelled engine done by comparing their respective BTE. Figure 4 shows variation of BTE with respect to load at

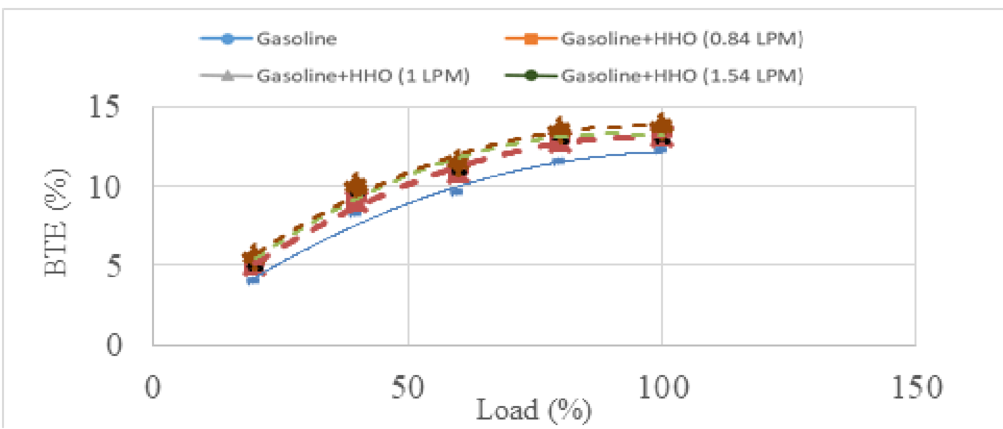

Figure 4 BTE variation with respect to load for different HHO flow rate.

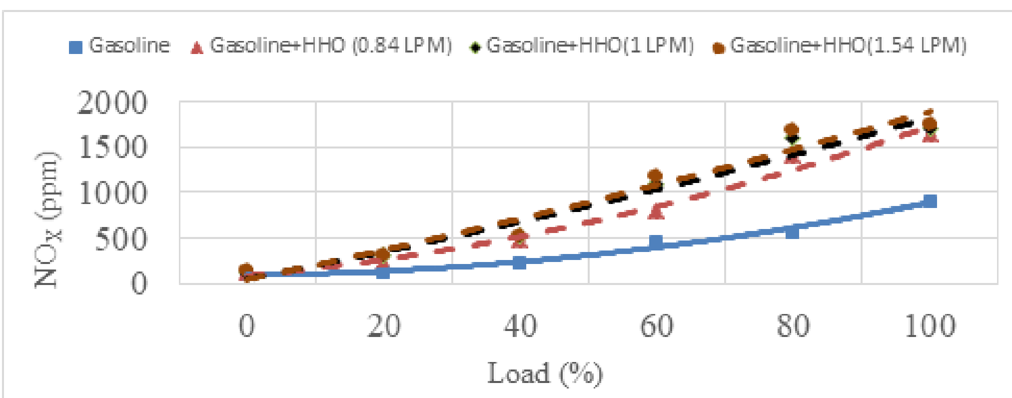

Figure 5. Variation of NOx emission with respect to load at different HHO flow rate.

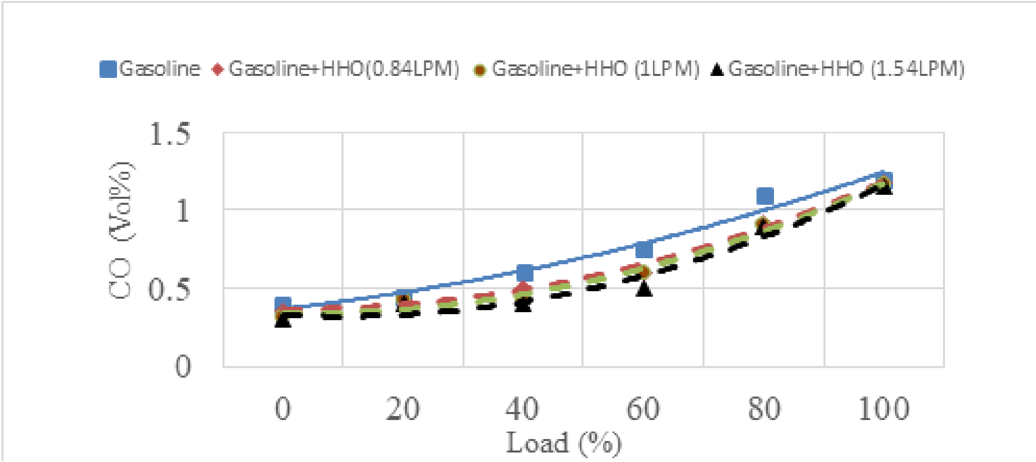

Figure 6. Variation of CO emission with respect to load at different HHO flow rate.

different HHO flow rate. BTE increases with increasing load and HHO flow rate, because as the load increases both fuel consumption and BP of the engine increases but rate of increase in BP supersedes rate of fuel consumption, which results in increase of BTE. Presence of hydrogen in the fuel mixture causes increase in flame speed and combustion efficiency which obviously increases BTE of the engine. Generally, BTE is maximum around 90% load but part loads which are the integer multiple of 20% is only possible, achieving all combinations of loads are impossible hence efficiency is shown to be maximum at full (100%) load. NO_x emission mainly depends on two factors namely equivalence ratio and temperature of combustion. An increase in load causes the fuel to be used more and the fuel mixture to become somewhat richer, which raises the emission of NOx.

Addition of HHO causes a rise of flame temperature of combustion due to the presence of hydrogen in the fuel mixture. At Higher temperatures reactivity between nitrogen and oxygen molecules was also greater, leading to a significant output of NOx. Figure 5 represents variation of NO_x emission against varying load and HHO flow rate. Figure 6 represents variation of CO emission against varying load at different HHO flow rate. The quantity of fuel used every cycle rises with increasing load, increasing CO emissions in the process. Presence of hydrogen in fuel mixture causes better combustion and low emission of CO, hence at low load and high HHO flow rate we can expect low emission of CO.

6.2 Simulation Results

6.2.1 In-Cylinder Pressure and Zonal Temperature

Figure 7 compares variation of in cylinder pressure of SI engine for both experimental [Ferguson *et al.*,[18]] and simulated values at rated load and 3000 RPM speed against crank angle. Simulated values are in well agree with the experimental values, but experimental peak pressure shows 61.5 bar while simulated results shows 65 bar almost at the same crank angle of 13.6^o ATDC. The variation in results is due to various assumptions made during the simulation. Figure 8 represents zonal temperature variation with respect to crank angle. The combustion chamber of the SI engine is divided into two zones: An unburned zone and a burned zone. Since pressure is uniform throughout the combustion chamber but volume and mass burned fractions are different for two zones, we can definitely expect two distinct temperature profiles for them. Current simulated outcomes were compared with simulated results from Ferguson *et al.*,[18]. The unburned temperature very well agrees with the previous results, but we can see a clear discrepancy in the burned temperature because the initial burned (adiabatic) temperature value is different for both simulation cases. Since IVP kind of differential equations were solved, we can expect different burned temperature profiles.

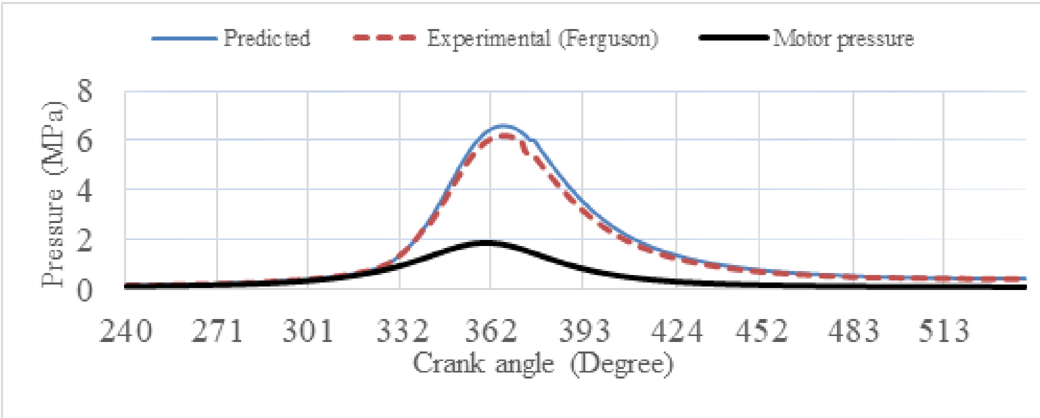

Figure 7. Variation of pressure with respect to crank angle.

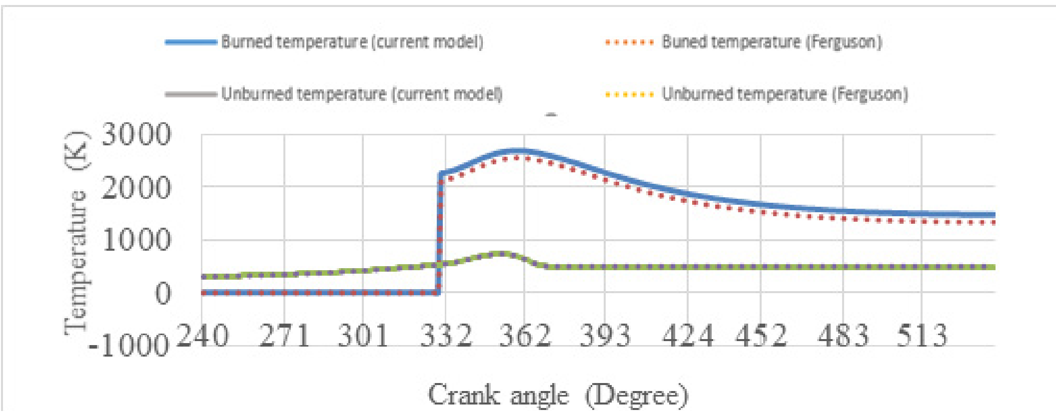

Figure 8. Variation of zonal temperature with respect to crank angle.

6.2.2 Mass Fraction Burned

Figure 9 compares predicted and experimental burned mass fraction against crank angle for pure gasoline combustion case. Here crank angles are taken from SOC (25° BTDC) to EOC where burned mass fraction equals to 1. Results show that both the results are in very good agreement with each other. Generally burned mass fraction follows 'S' curve, which signifies that at the initial

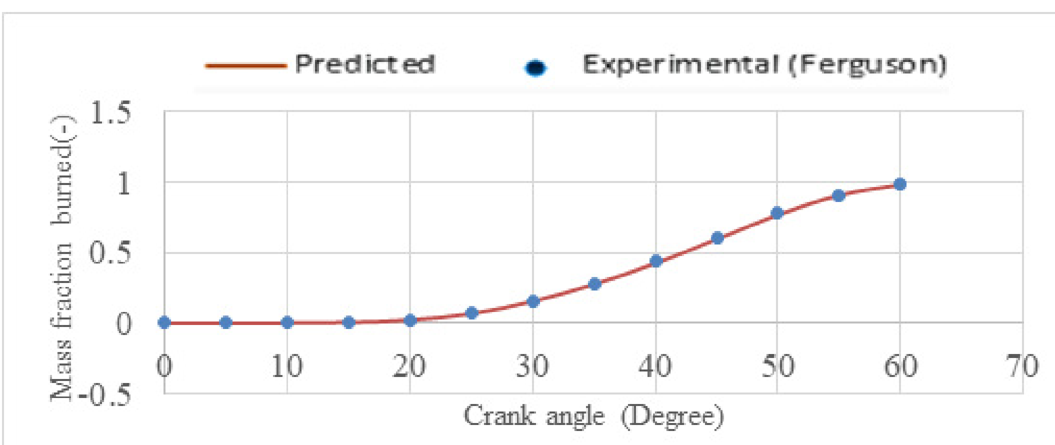

Figure 9. Variation of burned mass fraction with respect to crank angle.

and final phase of combustion, mass burn rate is low because of low turbulency and low availability of air-fuel mixture while at the intermediate phase there is a good amount of air-fuel mixture is available as well as high turbulency results in large mass burn rate.

7.0 Conclusions

- Usage of water electrolyser to produce HHO gas was found to be effective since it is efficient, economical and can generate HHO on demand.
- Maximum HHO fuel flow rate of 1.54 lpm was obtained which corresponds to 20 V (10 sets of plates).
- Corresponding to maximum HHO fuel flow rate 1.54 lpm, BTE and NO_x emissions increased by 1.75% and 800 ppm respectively at full load, while for the same set of conditions CO emission dropped by 0.25%.
- A two zone quasi-dimensional combustion model was developed using MATLAB software, and the results were compared with experimental values. Analysis showed that both numerical and experimental results are well in agreement with each other with a small discrepancy.
- Improvement in BTE is also supported by modelling results, presence of hydrogen in gasoline and HHO fuel mixture increases the turbulent flame speed (Equations (14) and (16)) and mass burn rate (Equation (13)), which in turn affects the rate of pressure rise (Equation (5)), which causes improvement in IMEP of the engine thus improves BTE and BP of the engine. These obtained findings might be helpful to fuel industries for declining CO emissions.

8.0 References

1. Iulianelli A, Basile A, editors. Advances in hydrogen production, storage and distribution. Elsevier; 2014.
2. Santilli RM. A new gaseous and combustible form of water. International Journal of Hydrogen Energy. 2006; 31(9):1113-28. https://doi.org/10.1016/j.ijhydene.2005.11.006
3. El Soly AK, El Kady MA, Farrag AE, Gad MS. Comparative experimental investigation of oxyhydrogen (HHO) production rate using dry and wet cells. International Journal of Hydrogen Energy. 2021; 46(24):12639-53. https://doi.org/10.1016/j.ijhydene.2021.01.110
4. Nikolic VM, Tasic GS, Maksic AD, Saponjic DP, Miulovic SM, Kaninski MP. Raising efficiency of hydrogen generation from alkaline water electrolysis- Energy saving. International Journal of Hydrogen Energy. 2010; 35(22):12369-73. https://doi.org/10.1016/j.ijhydene.2010.08.069
5. Apostolescu N, Chiriac R. A study of combustion of hydrogen-enriched gasoline in a spark ignition engine. SAE Transactions. 1996; 718-29. https://doi.org/10.4271/960603 PMid:23935691
6. El-Kassaby MM, Eldrainy YA, Khidr ME, Khidr KI. Effect of Hydroxy (HHO) gas addition on gasoline engine performance and emissions. Alexandria Engineering Journal. 2016; 55(1):243-51. https://doi.org/10.1016/j.aej.2015.10.016
7. Subramanian B, Lakshmaiya N, Ramasamy D, Devarajan Y. Detailed analysis on engine operating in dual fuel mode with different energy fractions of sustainable HHO gas. Environmental Progress and Sustainable Energy. 2022; 41(5):e13850. https://doi.org/10.1002/ep.13850
8. Kumar GA, Rao GV. Performance characteristics of oxy hydrogen gas on two stroke petrol engine. International Journal of Engineering Trends and Technology. 2013; 6(7):358-66.
9. Poulos SG, Heywood JB. The effect of chamber geometry on spark-ignition engine combustion. SAE transactions. 1983: 1106-29. https://doi.org/10.4271/830334 PMid:35651827
10. Buttsworth DR. Spark ignition internal combustion engine modelling using Matlab; 2002.
11. Blizard NC, Keck JC. Experimental and theoretical investigation of turbulent burning model for internal combustion engines. SAE Transactions. 1974; 846-64. https://doi.org/10.4271/740191 PMid:34778203
12. Tabaczynski RJ, Ferguson CR, Radhakrishnan K. A turbulent entrainment model for spark-ignition engine combustion. SAE Transactions. 1977:2414-33. https://doi.org/10.4271/770647 PMid:34899429
13. Wang S, Ji C. Cyclic variation in a hydrogen-enriched spark-ignition gasoline engine under various operating conditions. International Journal of Hydrogen Energy. 2012; 37(1):1112-9. https://doi.org/10.1016/j.ijhydene.2011.02.079
14. Yu G, Law CK, Wu CK. Laminar flame speeds of hydrocarbon+ air mixtures with hydrogen addi-

tion. Combustion and Flame. 1986; 63(3):339-47. https://doi.org/10.1016/0010-2180(86)90003-9

15. Paykani A, Frouzakis CE, Schürch C, Perini F, Boulouchos K. Computational optimization of $CH_4/H_2/CO$ blends in a spark-ignition engine using quasi-dimensional combustion model. Fuel. 2021; 303:121281. https://doi.org/10.1016/j.fuel.2021.121281
16. Sok R, Yamaguchi K, Kusaka J. Prediction of ultra-lean spark ignition engine performances by quasi-dimensional combustion model with a refined laminar flame speed correlation. Journal of Energy Resources Technology. 2021; 143(3):032306. https://doi.org/10.1115/1.4049127
17. Thermodynamics and Fluid Mechanics Group, Annand WJ. Heat transfer in the cylinders of reciprocating internal combustion engines. Proceedings of the Institution of Mechanical Engineers. 1963; 177(1):973-96. https://doi.org/10.1243/PIME_PROC_1963_177_069_02
18. Ferguson CR, Kirkpatrick AT. Internal combustion engines: Applied thermosciences. John Wiley & Sons; 2015.
19. Medina A, Curto-Risso PL, Hernández AC, Guzmán-Vargas L, Angulo-Brown F, Sen AK. Quasi-dimensional simulation of spark ignition engines. Thermodynamic Optimization to Cyclic Variability. London, UK; Springer; 2014. https://doi.org/10.1007/978-1-4471-5289-7
20. Heywood JB. Internal Combustion Engine Fundamentals. McGraw. Hill Book Company; 1988.

Nomenclature

ATDC	After Top Dead Centre
Ac	Alternating Current
BTE	Brake Thermal Efficiency
BTDC	Before Top Dead Centre
CNG	Compressed Natural Gas
BSFC	Brake Specific Fuel Consumption
bhp	Brake Horse Power
CO	Carbon Monoxide
DC	Direct Current
EOC	End of Combustion
HHO	Oxy-Hydrogen Gas Mixture
KOH	Potassium Hydroxide
LPG	Liquefied Petroleum Gas
lpm	Litres per minute
ppm	Parts per million
NaOH	Sodium Hydroxide
NO_x	Oxides of Nitrogen
RPM	Rotations per Minute
SI	Spark Ignition
SOC	Start of Combustion

UBHC	Unburned Hydrocarbon
A_f	Flame Front Area
C_p	Specific Heat at Constant Pressure
f	Phenomenological factor
h	Enthalpy
h_g	Heat transfer coefficient
m	mass
N	Rotational speed
P	Pressure
Q_w	Heat energy transfer to wall
R	Characteristic gas constant
S	Speed
T	Temperature
V	Velocity/Voltage/Volume
b	Burned
d	Displacement/swept
l	Laminar
m	Motor
mb	Burned mass
r	Reference
sto	Stoichiometric
t	Turbulent
u	Unburned
wu	Wall in contact with unburned zone
wb	Wall in contact with burned zone
α, β	Constants
ρ	Density